Dyes and Pigments 82 (2009) 329–335

Contents lists available at ScienceDirect

Dyes and Pigments

journal homepage: www.elsevier.com/locate/dyepig

The synthesis and photo-physical properties of a hemicyanine dye

Chuanxiang Qin [a,b], Xiaomei Wang [b], Jian-Jun Wang [b], Jiayuan Mao [b], Junyi Yang [c], Lixing Dai [b], Guoqiang Chen [a,*]

[a] College of Textile and Clothing Engineering, Soochow University, Suzhou 215021, China
[b] College of Chemistry, Chemical Engineering and Materials Science, Soochow University, Suzhou 215123, China
[c] School of Physical Science and Technology, Soochow University, Suzhou 215006, China

ARTICLE INFO

Article history:
Received 18 November 2008
Received in revised form
21 January 2009
Accepted 5 February 2009
Available online 15 February 2009

Keywords:
Hemicyanine dye
Single-photon absorption
Single-photon emission fluorescence
Non-linear optical absorption
Solvent effect
Z-scan

ABSTRACT

The hemicyanine dye, trans-4-[p-(*N*,*N*-di(2-hydroxyethyl))amino-styryl]-*N*-octylpyridinium tetraphenylborate (DHEASPT-C_8), was synthesized and characterized using ^{1}H NMR, thermo-analysis and elemental analysis. The linear optical properties in several solvents were measured using UV–vis as well as single-photon spectrophotometer, while the non-linear optical properties in DMF were measured using the Z-scan technique at 532 nm using 4 ns pulsed laser. The influence of the dye anion on its optical properties was investigated by comparing DHEASPT-C_8 to trans-4-[p-(*N*,*N*-hydroxyethyl)amino-styryl]-*N*-octylpyridinium bromide (DHEASPBr-C_8), from which it was observed that there were blue shifts in both single-photon absorption spectra and fluorescence spectra. Z-scan measurements showed that DHEASPBr-C_8 displayed saturable absorption with less obvious refractive phenomena, while DHEASPT-C_8 had reverse saturable absorption with obvious refractive phenomena. For DHEASPT-C_8, the NLO absorption coefficient β was 3.09×10^{-11} m/W and the third-order NLO coefficient $\chi^{(3)}$ was 4.78×10^{-12} esu.

1. Introduction

Hemicyanine dyes are types of important functional dyes and have applications in optical power limiting [1], two-photon pumped upconversion intracavity lasing [2], fluorescence probes [3], fluorescent thermometer [4], molecular electronics [5,6], Langmuir film [7–9], and photoinitiated polymerization [10]. The authors have studied the synthesis, molecular engineering and optical properties of some hemicyanine dyes in the past decade [11–14]. In terms of molecular engineering, structural features such as the π-conjugation style, molecular planarity and the length of the conjugated bridge play important roles in the optical properties of optical materials [15–18]. Among the hemicyanine dyes, trans-4-[p-(*N*,*N*-hydroxyethyl)amino-styryl]-*N*-octylpyridinium bromide (DHEASPBr-C_8) is reported to display good optical properties, possessing stronger single-photon absorption and two-photon absorption spectrogram, for the highly conjugated cation (i.e. DHEASP-C_8^+) [13,14]. Moreover, DHEASPBr-C_8 has good compatibility with polymeric matrixes and polyimide film prepared from DHEASPBr-C_8-doped poly(amic acid) solution had clear single-photon absorption and two-photon absorption properties. However, DHEASPBr-C_8 was found to have poor solubility in common organic solvents (e.g. THF, acetone and ethyl acetate) and its application in fields where such solvents are used is restricted. Recently, the authors synthesized another hemicyanine dye (i.e. DHEASPT-C_8) by replacing the bromide ion (Br^-) with a bulky anion (tetraphenylborate ion, BPh_4^-); DHEASPT-C_8 was soluble in such solvents. To explore the importance of the anion in such a hemicyanine dye, the characteristics of DHEASPBr-C_8 and DHEASPT-C_8 were investigated; their molecular structures are shown in Fig. 1.

2. Experimental

2.1. Materials

N-Phenyldiethanolamine was purchased from Acros Organic and used without further purification. Other solvents (A.R.) and reagents were obtained commercially and used without further purification except for dimethylformamide (DMF), ethanol and methanol. DHEASPBr-C_8, as substrate for the synthesis of DHEASPT-C_8, was synthesized following Ref. [13]. The exact synthetic procedure is shown in Fig. 2.

2.2. Synthesis

2.2.1. 4-[N,N-Bis(2-hydroxyethyl)amino]benzaldehyde (compound **1**)

Yield 62% and mp 60 °C. IR (KBr pellet, cm^{-1}): 3376.1 (–OH), 1655.7 (C=O), 1595.7 and 1578.8 (Ar-CH), 1173.2 (C–O), ^{1}H NMR

* Corresponding author. Tel./fax: +86 512 6716 2166.
E-mail address: chenguojiang@suda.edu.cn (G. Chen).

0143-7208/$ – see front matter © 2009 Elsevier Ltd. All rights reserved.
doi:10.1016/j.dyepig.2009.02.002

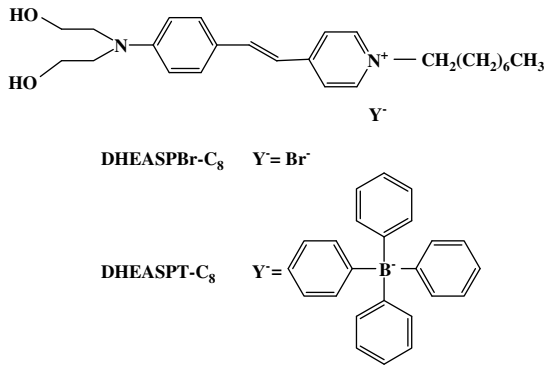

Fig. 1. Molecular structures of DHEASPBr-C_8 and DHEASPT-C_8.

($CDCl_3$, 400 Hz) δ: 9.56 (1H, –CHO, s), 7.61 (2H, Ar-CH, d, *J* 8.8 Hz), 6.66 (2H, Ar-CH, d, *J* 9.2 Hz), 4.52 (2H, –OH, s), 3.85 (4H, $-CH_2-$, t, *J* 5.0 Hz), 3.64 (4H, $-CH_2-$, t, *J* 5.0 Hz).

2.2.2. 4-Methyl-N-n-*octylpyridinium bromine (compound **2**)*

Yield 65% and mp 83 °C. IR (KBr pellet, cm^{-1}): 1641.4 and 1469.6 (Ar-CH and C–N), ^1H NMR ($CDCl_3$, 400 Hz) δ: 9.35 (d, 2H, Py-CH, *J* 6.6 Hz), 7.91 (d, 2H, Py-CH, *J* 6.3 Hz), 4.92 (t, 2H, Py $-CH_2-$, *J* 7.4 Hz), 2.68 (s, 3H, CH_3-), 2.01 (q, 2H, $-CH_2-$), 1.33 (q, 4H, $-CH_2-$), 1.23 (q, 6H, $-CH_2-$), 0.86 (t, 3H, $-CH_3$, *J* 6.6 Hz). Elemental analysis: Calcd C, 62.89; H, 7.81; N, 5.87. Found: C, 62.48; H, 7.57; N, 5.56.

*2.2.3. Trans-4-[p-(*N,N-*hydroxyethyl)amino-styryl]*-N-*octylpyridinium bromide (DHEASPBr-C_8)*

Yield 69% and T_d 298.0 °C. ^1H NMR (DMSO-d_6, 400 MHz) δ: 8.80 (2H, Py-CH, d, *J* 6.9 Hz), 8.08 (2H, Py-CH, d, *J* 6.6 Hz), 7.92 (1H, CH═CH, d, *J* 15.9 Hz), 7.58 (2H, Ar-H, d, *J* 9.0 Hz), 7.16 (1H, CH═CH, d, *J* 16.2 Hz), 6.81 (2H, Ar-H, d, *J* 9.0 Hz), 4.44 (2H, Py $-CH_2-$, t, *J* 7.5 Hz), 3.55 (8H, $-CH_2-$, q), 1.27–1.24 (10H, $-CH_2-$, q), 1.16 (2H, $-CH_2-$, q), 0.85 (3H, $-CH_3$, t, *J* 7.05 Hz). Elemental analysis: Calcd C, 62.89; H, 7.81; N, 5.87. Found: C, 62.48; H, 7.57; N, 5.56.

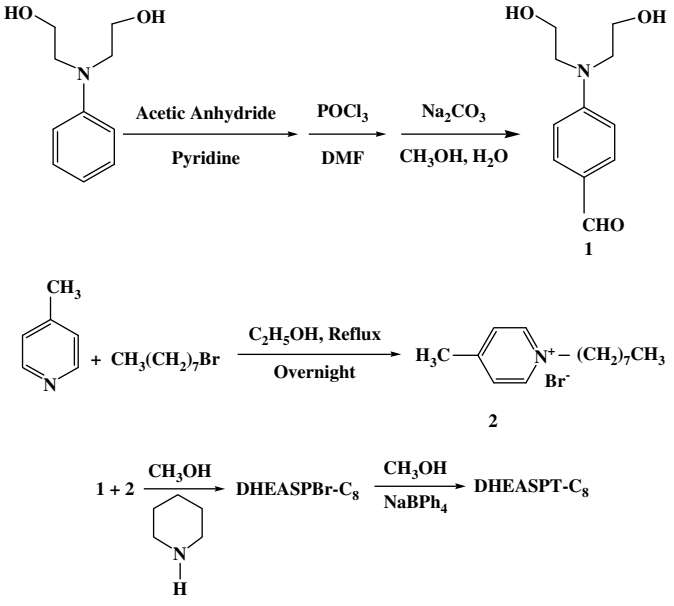

Fig. 2. Route for the synthesis of DHEASPT-C_8.

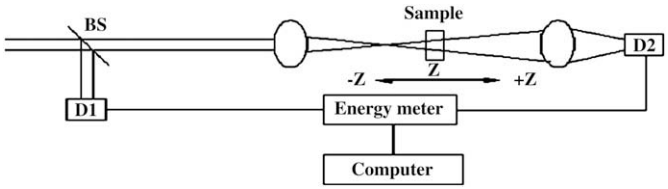

Fig. 3. Open-aperture Z-scan apparatus.

*2.2.4. Trans-4-[p-(*N,N-*di(2-hydroxyethyl))amino-styryl]*-N-*octylpyridinium tetraphenylborate (DHEASPT-C_8)*

To a solution of DHEASPBr-C_8 (0.03 mol, 14.3 g) in methanol (200 mL) was added dropwise a solution of sodium tetraphenylborate (10.3 g, 0.03 mol) in methanol (100 mL). Several hours later, a red precipitate was formed and washed with methanol several times, collected by filtration and then dried.

Yield 56% and T_m 48.3 °C. ^1H NMR (DMSO-d_6, 400 MHz) δ: 8.75 (2H, Py-CH, d, *J* 6.0 Hz), 8.07 (2H, Py-CH, d, *J* 6.4 Hz), 7.91 (1H, CH═CH, d, *J* 19.2 Hz), 7.60 (2H, Ar-H, d, *J* 7.6 Hz), 7.22 (1H, CH═CH, d, *J* 16.0 Hz), 7.18–6.93 (20H, Ar-H, q), 6.83 (2H, Ar-H, d, *J* 8.8 Hz), 4.28 (4H, $-CH_2-$, t, *J* 5.8 Hz), 3.71 (4H, $-CH_2-$, t, *J* 5.8 Hz), 1.57 (2H, $-CH_2-$, m), 1.25 (12H, $-CH_2-$, m), 0.88 (3H, $-CH_3$, t, *J* 6.2 Hz). Elemental analysis: Calcd C, 82.10; H, 8.02; N, 3.91. Found: C, 81.95; H, 7.94; N, 3.67.

2.3. Measurements

The ^1H NMR spectra were recorded with a GCT-TOF NMR spectrometer at 400 MHz. Dimethylsulfoxide (DMSO) and deuterated chloroform ($CDCl_3$) were used as solvents, respectively, and tetramethylsilane (TMS) as the internal standard. IR spectra were measured on a Nicolet 5200 FT-IR 5DX instrument using solid samples dispersed in KBr pellets. The melting points and decomposition temperatures were measured on a Perkin–Elmer Diamond 5700 thermo-gravimetric analyzer at a heating rate of 20 °C/min under a nitrogen atmosphere.

UV–vis absorption spectra were recorded at room temperature in quartz cells of 1 cm path length using a TU-1800 SPC spectrophotometer, and then single-photon emission fluorescence spectra were obtained in the same cell under excitation of the respective maximum absorption wavelength on an Edinburgh 920 spectrofluorometer. In this study, all of the concentrations of the dye solutions in the linear spectra were 1.0×10^{-5} M, as no aggregation or self-absorption effects of dyes were observed at this concentration [19]. The reference standard used for quantum yield determination was 4-(dicyanomethylene)-2-methyl-6-(p-(dimethylamino) styryl)-4*H*-pyran (DCM) (1.0×10^{-5} M) in THF solution ($\Phi = 0.5$).

To measure the optical non-linearity, open/close aperture Z-scan measurements were performed at 532 nm using 4 ns laser pulses from a Nd:YAG laser (EKSPLA) [20,21]. DHEASPBT-C_8 was dissolved in DMF solution (2.0×10^{-5} M) and placed in a 2 mm quartz cuvette for NLO measurements. In the open-aperture Z-scan, depicted in Fig. 3, the laser beam was focused using a lens with $f = 400$ mm focal length, and the sample was translated along the beam axis (*z*-axis) through the focal region ($z = 0$) over a distance several times that of the diffraction length. At each position z the sample sees different laser intensity, and the incident and transmitted pulse energies were simultaneously measured using two energy detectors linked to an energy meter. Laser pulses were fired at a repetition rate of 2 Hz, and the data acquisition was automated. The pulse energy reaching the sample was approximately 25 μJ.

3. Results and discussion

3.1. Synthesis of dyes and the solvability of two hemicyanine dyes

The ^{1}H NMR spectra of DHEASPT-C_8 displayed two characteristic doublets localized at chemical shifts of 7.22 and 7.91 ppm. Both were attributed to vinyl hydrogen atoms. Based on the large coupling constant for the olefinic proton ($J = 16$–19), it was concluded that DHEASPT-C_8 existed as the all-trans conformation in the ground state [22].

The solubility of the two dyes was tested in several solvents. DHEASPBr-C_8 could dissolve easily in ethanol and H_2O, but not in routine organic solvent (i.e. THF, acetone). DHEASPT-C_8 could dissolve easily in THF and acetone, but not in ethanol and H_2O. So the anion in the dyes had a great influence on the solubility, and this property is very important in their further application.

3.2. Optimized geometry of the two hemicyanine dyes

In this paper, the influence of the anion in hemicyanine dye molecule upon optical behaviors would be discussed. The optimized conformations of the hemicyanine dye in the presence of two anions, obtained with the Hyperchem program, showed that the stilbene subunits in both samples were approximately planar (seen in Fig. 4), and they were asymmetric chromophores. But BPh_4^- on the terminal of DHEASPT-C_8 had larger physical dimensions and a greater steric effect than Br^- on the terminal of DHEASPBr-C_8, which in turn would have some influence on the optical properties.

3.3. Spectroscopic studies

3.3.1. Linear optical properties

Both dyes are composed by a donor group of electrons (dimethylamino group) and an acceptor group of electrons (pyridinium moiety) connected by an ethylene chain with delocalized p-electrons [8]. Generally, the photophysics of this kind hemicyanine dye in solution can be compared with the photophysics of the similar molecule DEASPI (trans-4-[p-(*N*,*N*-diethylamino) styryl]-*N*-methylpyridinium iodide) or more generally push–pull stilbenes. The linear absorption and single-photon emission fluorescence (OPF) spectra of the two dyes in DMF solvent are shown Fig. 5. Both dyes showed stronger spectrum character curve when the dye concentration in DMF solvent was 1×10^{-5} M, for the stilbene subunits in both dyes were approximately planar (shown in Fig. 4), which were beneficial to the intra-molecular charge transfer between donor and acceptor. However, the maximum absorption peaks showed

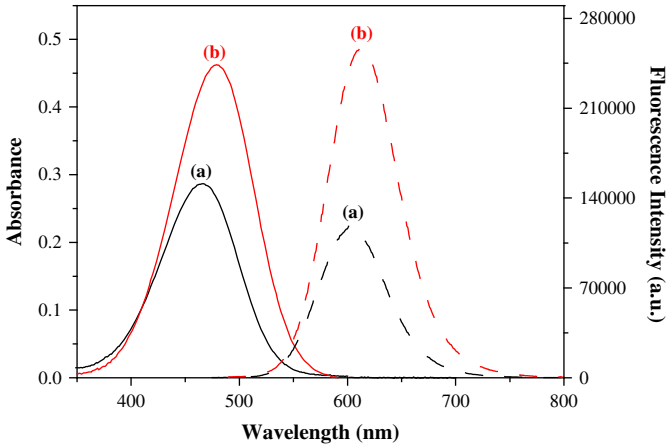

Fig. 5. Linear absorption (solid) and single-photon fluorescence spectra (dashed) of samples in DMF solvent at $d_0 = 1 \times 10^{-5}$ M (a) DHEASPT-C_8, (b) DHEASPBr-C_8.

a blue shift of 13 nm going from DHEASPBr-C_8 ($\lambda_{max}^{ab} = 479$ nm) to DHEASPT-C_8 ($\lambda_{max}^{ab} = 466$ nm). At the same time, the OPF peak showed a blue shift of 12 nm going from DHEASPBr-C_8 ($\lambda_{max}{}^{em} = 613$ nm) to DHEASPT-C_8 ($\lambda_{max}^{em} = 601$ nm) under excitation with the respective maximum absorption wavelength. It was also found that DHEASPT-C_8 possessed weaker fluorescence emission intensity than DHEASPBr-C_8. Choi et al. have mentioned that a bulky anion (tetraphenylborate) was substituted for bromide anion at the salt unit in order to reduce the ionic mobility and then allowed the polymer to be efficiently poled [23]. Then $BPh4^-$ is more stable in DHEASPT-C_8 and may reduce the acceptor ability of pyridinium moiety in the push–pull structure, resulting in a blue shift and less fluorescent intensity than that of DHEASPBr-C_8.

The quantum yield of the tested dye (Φ_{dye}) in different solvents was calculated using Eq. (1)

$$\Phi_{dye} = \Phi_{ref} \frac{I_{dye} A_{ref}}{I_{ref} A_{dye}} \frac{n_{dye}^2}{n_{ref}^2} \quad (1)$$

where Φ_{ref} (=0.5) and n_{ref} (=1.4073) are the fluorescence quantum yield of DCM and the optical refractive index of THF solvent, respectively, n_{dye} is the refractive index of the tested solvent, A_{ref} and A_{dye} are the absorbance values for DCM and tested dye, respectively, and I_{ref} and I_{dye} are the areas' integral values of the corrected fluorescence spectra for DCM and tested dye, respectively.

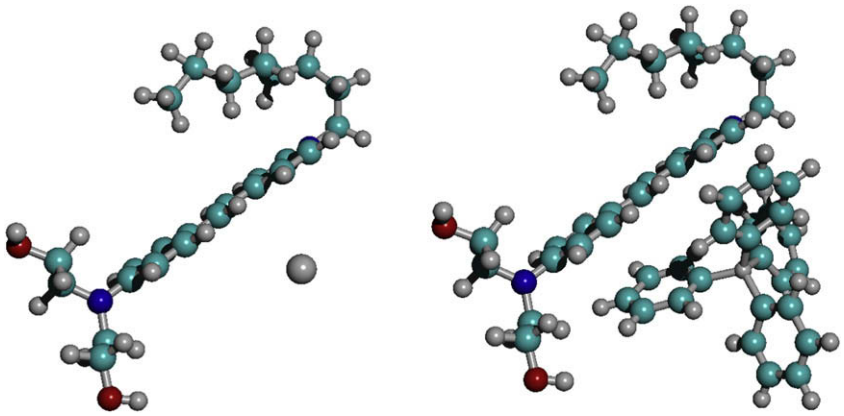

Fig. 4. Optimized geometry of DHEASPBr-C_8 (left) and DHEASPBT-C_8 (right).

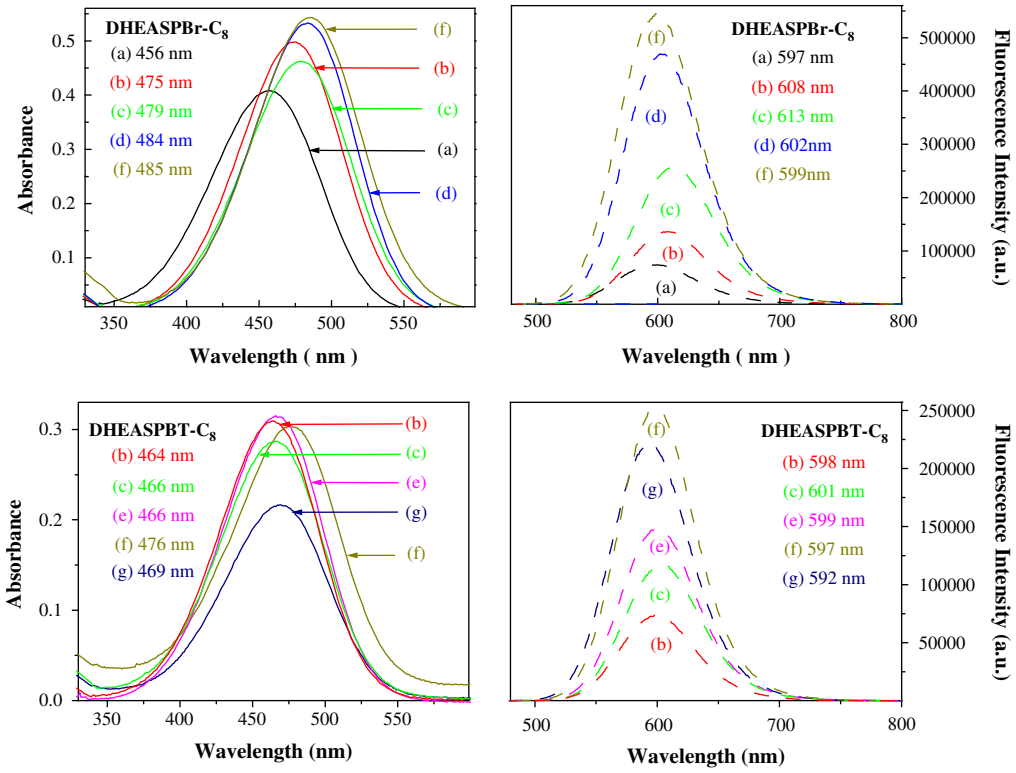

Fig. 6. Linear absorption (solid) and single-photon fluorescence spectra (dashed) of DHEASPBr-C_8 and DHEASPT-C_8 in different solvents at $d_0 = 1 \times 10^{-5}$ M. ((a) H_2O, (b) CH_3CN, (c) DMF, (d) C_2H_5OH, (e) acetone, (f) THF, (g) ethyl acetate).

As seen from Fig. 6 and Table 1, the fluorescence intensities and fluorescence quantum yield (Φ) of the two dyes were inclined to decrease with the increase in solvent polarity. Based on the "twisted intra-molecular charge transfer" (TICT) model [25], the larger solvent polarity and the more obvious solvation for the non-emissive "TICT" state of chromophore, dyes gave lower fluorescence intensities in more highly polar solvents such as CH_3CN.

The data in Table 1 indicates that this kind of hemicyanine dye is a solvatochromic dye. Generally, the solvatochromic shifts were processed by applying the Lippert–Mataga equation [26].

$$hc(\nu_{abs} - \nu_{em}) = \frac{1}{4\pi\varepsilon_0}\frac{2}{a^3}\mu_e\left(\mu_e - \mu_g\right)\Delta f + \text{const} \tag{2}$$

$$\Delta f = \frac{\varepsilon - 1}{2\varepsilon + 1} - \frac{(n^2 - 1)}{(2n^2 + 1)} \tag{3}$$

where μ_e and μ_g are the dipole moments in the excited and ground state, respectively, $(\nu_{abs} - \nu_{em})$ is the Stokes shift, ε is the dielectric constant, n is the optical refractive index, and Δf is the solvent polarity function.

Based on Table 1, the Lippert–Mataga plots for DHEASPBr-C_8 and DHEASPT-C_8 are shown in Fig. 7. It was found that each slope was greater than zero, so μ_e was larger than μ_g. That is the excited state is more polar than the ground state. Then the ground state of a particular molecule may change very little from solvent to solvent, but the excited state may be quite different because of its dipole moment. If the difference between the Franck–Condon (FC) excited state and the equilibrium-excited state in the non-polar solvent is greater than the difference between FC excited state and the equilibrium-excited state for polar solvent, the fluorescence spectrum will be to the red and the energy of the equilibrium-excited state in the non-polar solvent is less than that of the equilibrium-excited state in the polar solvent [27]. DHEASPBr-C_8 and DHEASPT-C_8 are pyridinium salts containing character cations and anions and they are easy to form stable complex with polar solvent in ground state for electrostatic attraction, which may increase the energy difference (ΔE) of HOMO – LUMO, resultant equilibrium-excited state level shifts to a higher energy in the polar solvent. Then the energy of the equilibrium-excited state in the non-polar solvent is less than that of the equilibrium-excited state in the polar solvent and the fluorescence spectra were inclined to red shift as the solvent dipole moment ($\mu/10^{-30}$ C m) increased as the asymmetric dye PSPI (trans-4-(p-pyrrolidinyl styryl)-*N*-methylpyridinium iodide) mentioned before [12].

For further comparison of the different anions, the slopes were calculated and one could see that the solvent effect in DHEASPT-C_8 was weaker than that in DHEASPBr-C_8. This might be attributed to the special structure of BPh_4^- and the dipole moment gap (μ_e ($\mu_e - \mu_g$)) of DHEASPT-C_8 was lower. Hemicyanine dyes exhibit a significant charge displacement when the molecules are excited from the ground state to an excited state and this large charge displacement is an indication for a large polarizability [6]. Because the ionic mobility of BPh_4^- is inferior to that of Br^- and DHEASPT-C_8 is more stable than DHEASPBr-C_8 in the solvent surroundings, the dipole moment gap (μ_e ($\mu_e - \mu_g$)) of DHEASPT-C_8 is lower than that of DHEASPBr-C_8.

However, the Lippert–Mataga plots obtained does not display a good linear dependence in the two dyes. The most obvious deviation of the spectroscopic result is observed when DHEASPBr-C_8 is solved in water. The departure from a linear Lippert–Mataga plot is an indication of specific interactions (for example, hydrogen bonding, and electron withdrawing-donating) between the dye and the solvent. In the case of this

Table 1
Spectral values of DHEASPBr-C_8 (a) and DHEASPT-C_8 (b) in different solvents at $d_0 = 1 \times 10^{-5}$ M [24].

Solvent	Ethyl acetate	THF	DMF	Acetone	Ethanol	CH_3CN	H_2O
ε	6.02	7.58	36.71	20.7	25.7	37.5	80.1
$\mu/10^{-30}$ C m[18]	6.27	5.70	12.88	8.97	5.60	11.47	6.47
Δf	0.1996	0.2095	0.2752	0.2852	0.2880	0.3054	0.3201
(a) $\nu_{abs} - \nu_{em}$ (cm^{-1})	–	3924.2	4563.6	–	4049.9	4605.3	5235.3
Φ	–	0.6088	0.3539	–	0.5041	0.1493	0.1010
(b) $\nu_{abs} - \nu_{em}$ (cm^{-1})	4430.1	4258.0	4764.7	4820.3	–	4829.3	–
Φ	0.5854	0.4827	0.2491	0.2556	–	0.1267	–

paper, it is clear that departure from linearity is a result of a strong hydrogen bonding. Since this kind dye differs from other hemicyanine dyes for it has a substitution of a hydroxyl group on the amino moiety. The influence of the hydroxyl group is significant in water, where the hydrogen bonding effect decreases the energy of the ground state [28], leading to a significant blue shift in the absorption (seen in Fig. 6), but also decreases the energy of the excited state, resulting in an extraordinarily large Stokes shift (seen in Table 1).

3.3.2. Non-linear optical properties

The properties of dye in DMF solution (2×10^{-5} M) were investigated with 532 nm laser pulses using the Z-scan technique [20]. Experimental results are demonstrated in Fig. 8. The square dots represent the Z-scan experimental data: Fig. 8a and c data collected under the open-aperture configuration, Fig. 8b and d data obtained by dividing the normalized Z-scan data obtained under the closed-aperture configuration by the normalized Z-scan data in Fig. 8a and c. The solid line represents 20 point adjacent averaging smoothing of the experimental data. The non-linearity of pure DMF solvent was also measured under the same conditions as the above cases, but no signal could be obtained, so the non-linearity of solvent can be ruled out.

In general, non-linear absorption of organic molecules can be easily explained using a five-level model involving S_0, S_1, S_2, T_1 and T_2. S_0, S_1, S_2, T_1, T_2 correspond to singlet and triplet manifolds, and each state contains a number of vibration levels [29]. Both molecules of the ground state and the excited state contribute to the absorption of the sample. Under the illumination of laser, some portions of molecules of the ground state S_0 are excited electronically from the lowest vibration level of S_0 to the upper vibration levels of S_1 and the molecules will arrive at lowest vibration level of S_1 very quickly by nonradiative decay. Molecules on the first excited state S_1 can be excited to S_2 by absorbing photon or relax to T_1 via intersystem crossing and the molecules on T_1 can be excited to T_2 finally. Non-linear absorption can be observed here. The two processes (S_1–S_2 and T_1–T_2) are known as excited states absorption (ESA), and if their absorption cross-sections are smaller (or larger) than that of the ground-states linear absorption, then these are referred to as saturable absorption (SA) (or reverse saturable absorption (RSA)). It can be seen in Fig. 8 that the normalized transmittance plotted as a function of the sample position (z) measured with open aperture is symmetrical with respect to $z = 0$. Fig. 8a and b shows that DHEASPBr-C_8 has saturable absorption (SA) but less obvious refractive phenomena, while Fig. 8c and d shows that DHEASPT-C_8 has both reverse saturable absorption (RSA) and obvious refractive phenomena with self-defocusing behavior. One can say that $BPh4^-$ make DHEASPT-C_8 have the larger excited states absorption cross-sections than that of the ground-states linear absorption.

In this work, only the NLO properties of DHEASPT-C_8 were calculated as the refractive behavior of DHEASPBr-C_8 was less obvious. The NLO absorption data were collected under an open-aperture configuration. The normalized transmission for the open aperture is given by Eqs. (4)–(7) [20,30–33], which is used to describe a third-order NLO absorptive process:

$$T(z, s = 1) = \sum_{m=0}^{\infty} \frac{[-q_0(z)]^m}{(m+1)^{3/2}} \quad \text{for } |q_0| < 1 \tag{4}$$

$$q_0(z) = \frac{\beta I_0 L_{\text{eff}}}{1 + z^2/z_0^2} \tag{5}$$

$$L_{\text{eff}} = \frac{1 - \exp(-\alpha_0 L)}{\alpha_0} \tag{6}$$

$$z_0 = \pi\omega_0^2/\lambda \tag{7}$$

Where β (m/W) is the NLO absorption coefficient, I_0 is the intensity at the focal point ($z = 0$), L_{eff} is the effective length of the sample, α_0 is the linear absorption coefficient of the sample and L is the sample thickness. z_0 is the Rayleigh length of the beam, where ω_0 is the spot radius of the pulse at focus and λ is the wavelength of the laser pulse.

The value of β could be obtained by fitting Eq. (4) to the measured data numerically shown in Fig. 8c. The obtained NLO absorption coefficient (β) of DHEASPBT-C_8 was 3.09×10^{-11} m/W.

The NLO refractive property of DHEASPBT-C_8, shown in Fig. 8d, was assessed by dividing the normalized Z-scan data obtained under closed-aperture configuration by the normalized Z-scan data obtained under open-aperture configuration. In Fig. 6d, the difference between the normalized transmittance values at valley and peak positions (ΔT_{P-V}) was related to the effective third-order NLO refractive index γ (m^2/W). γ could be derived from ΔT_{P-V} using Eq. (8) [32,33].

$$\gamma = \frac{\lambda \Delta T_{P-V}}{0.406(1-S)^{0.25}\pi I_0 L_{\text{eff}}} \tag{8}$$

where S is a parameter depending on the size of the aperture. The value of γ obtained was -6.01×10^{-18} m^2/W. On the other hand, the valley–peak pattern of the corrected transmittance curves showed self-defocusing behavior of the propagating light in the sample of DHEASPBT-C_8, i.e. negative γ. That is, the transmittance was less at the sample position behind the focal point ($z = 0$) than that in front of the focal point.

NLO processes are governed by the non-linear susceptibility ($\chi^{(3)}$) of NLO materials. The larger the $\chi^{(3)}$ value, the better the material's NLO properties. In accordance with the observed γ and β values, the modulus of the effective $\chi^{(3)}$ can be calculated from Eq. (9) [20,30–33].

$$\left|\chi^{(3)}\right| = \sqrt{\left(\chi_R^{(3)}\right)^2 + \left(\chi_I^{(3)}\right)^2} \text{ when } \chi_R^{(3)} = \frac{cn_0^2}{80\pi}\gamma;$$
$$\chi_I^{(3)} = \frac{9 \times 10^8 \varepsilon_0 c^2 n_0^2}{4\pi\omega}\beta \tag{9}$$

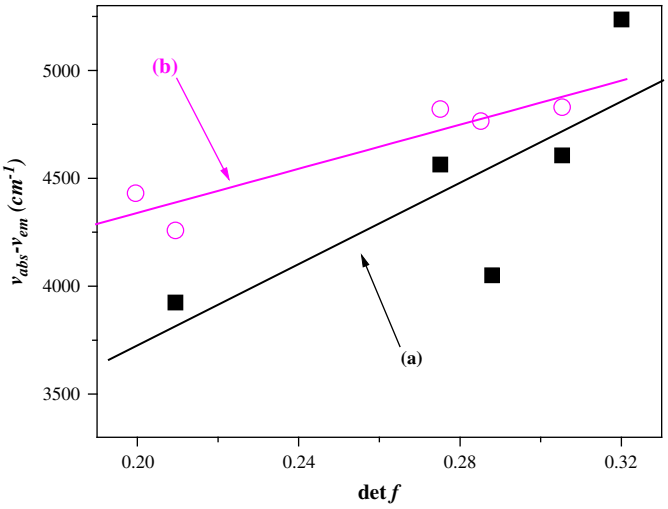

Fig. 7. Plots of Stokes shift ($\nu_{abs} - \nu_{em}$) vs. the solvent polarity function Δf (*det f*). (a) DHEASPBr-C_8 ($y = 1843.5 + 9412.6\ x$, $R^2 = 0.5958$), (b) DHEASPT-C_8 ($y = 3318.4 + 5106.4\ x$, $R^2 = 0.8629$).

where n_0 is the line refractive index of the sample, ε_0 is the permittivity of free space, and c is the velocity of light. Assuming that the non-linearity developed is predominantly of the third-order and the imaginary part of $\chi^{(3)}$ is due to non-linear absorption, the real part of $\chi^{(3)}$ is due to non-linear refraction.

In the experiment with DHEASPBT-C_8, the real part $\chi^{(3)}{}_R$ and the imaginary part $\chi^{(3)}{}_I$ of $\chi^{(3)}$ were -4.08×10^{-12} esu and 1.02×10^{-12} esu, respectively, and the experimentally determined value of $\chi^{(3)}$ was 4.78×10^{-12} esu. As a reference, the Z-scan tests on a sample of CS2 were also performed, and the obtained $\chi^{(3)}$ was 6.57×10^{-12} esu.

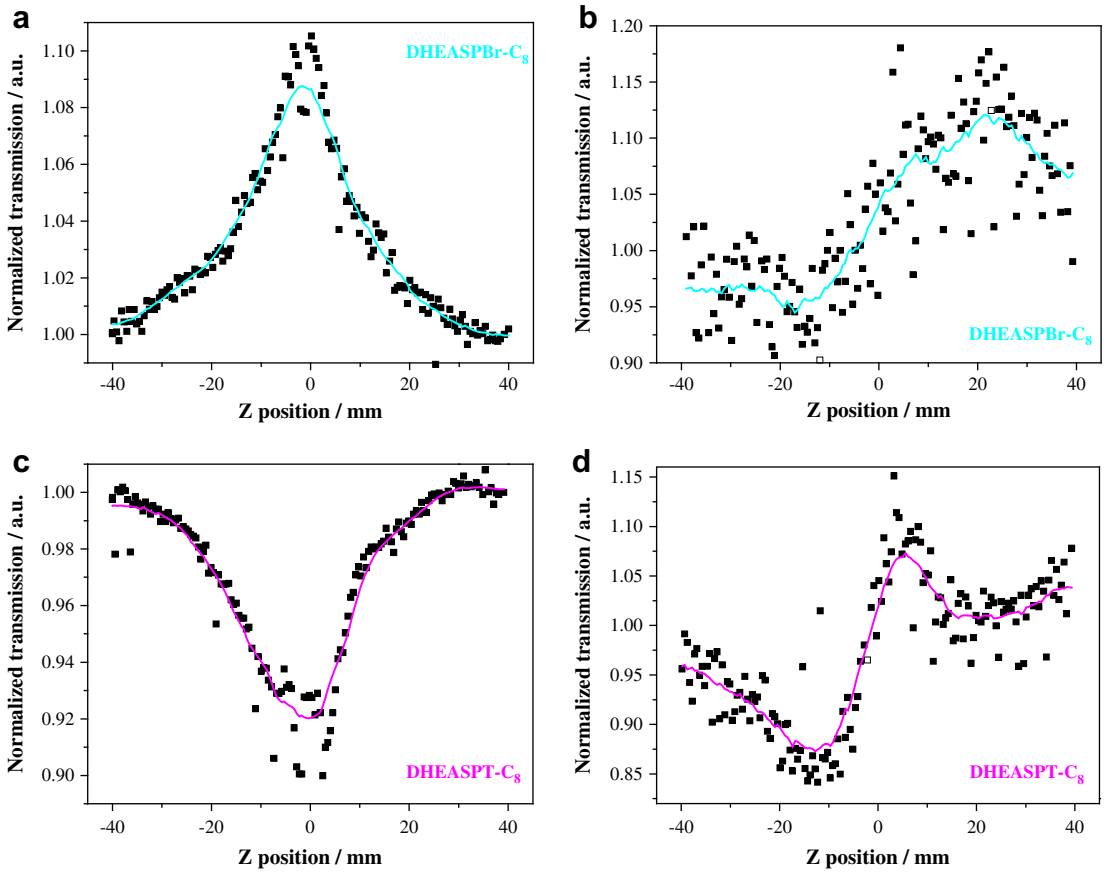

Fig. 8. Z-scan measurements of the two dyes in DMF solution (2×10^{-5} M) at 532 nm ((a, c) data collected under the open-aperture configuration; (b, d) data obtained by dividing the normalized Z-scan data obtained under the closed-aperture configuration by the normalized Z-scan data in (a, c)).

4. Conclusions

One hemicyanine dye, named DHEASPT-C_8, was synthesized successfully and its optical properties were studied. Its one photon emission fluorescence intensities were inclined to decrease with increasing solvent polarity based on the "twisted intra-molecular charge transfer" (TICT) model. While the fluorescence spectra were inclined to red shift as the solvent dipole moment increased for the equilibrium-excited state energy of this kind hemicyanine dye in the non-polar solvent is less than that of the equilibrium-excited state in the polar solvent. When DHEASPBT-C_8 is compared with DHEASPBr-C_8, the maximum absorption peaks show a blue shift and the fluorescence quantum yield (Φ) decrease in linear optical spectra. Meanwhile DEASPT-C_8 shows saturable NLO absorption whereas DHEASPBr-C_8 shows reverse saturable NLO absorption. The non-linear optical experimental results of DHEASPT-C_8 by the Z-scan technique at 532 nm showed that the NLO absorption coefficient β was 3.09×10^{-11} m/W and the third-order NLO coefficient $\chi^{(3)}$ was 4.78×10^{-12} esu.

Acknowledgements

The authors are grateful to the National Natural Science Foundation of China (Grant No. 50673071 and 50673020) for financial support.

References

[1] He GS, Bhawalkar JD, Zhao CF, Prasad PN. Optical limiting effect in a two-photon absorption dye doped solid matrix. Applied Physics Letters 1995;67:2433–5.
[2] He GS, Cui YP, Bhawalkar JD, Prasad PN, Bhawalkar DD. Intracavity upconversion lasing within a Q-switched Nd:YAG laser. Optics Communications 1997;133:175–9.
[3] Ephardt H, Fromherz P. Fluorescence and photoisomeriration of an amphiphiiic aminostiibazoiium dye as controlled by the sensitivity of radiationless deactivation to polarity and viscosity. Journal of Physical Chemistry 1989;93:7711–25.
[4] Shiraishi Y, Miyamoto R, Hirai T. A hemicyanine-conjugated copolymer as a highly sensitive fluorescent thermometer. Langmuir 2008;24:4273–9.
[5] Huang YY, Cheng TR, Li FY, Luo CP, Huang CH. Photophysical studies on the mono- and dichromophoric hemicyanine dyes II. Solvent effects and dynamic fluorescence spectra study in chloroform and in LB films. Journal of Physical Chemistry B 2002;106:10031–40.
[6] Kabatc J, Osmiałowski B, Paczkowski J. The experimental studies on the determination of the ground and excited state dipole moments of some hemicyanine dyes. Spectrochimica Acta Part A Molecular and Biomolecular Spectroscopy 2006;63:524–31.
[7] Han K, Wu YX, Tang G, Zhang GY, Wang Q, Li HP. Flow orientation and superquadratic dependence of second harmonic intensity on the film thickness in hemicyanine Langmuir–Blodgett multilayers. Optical Materials 2004;27:155–60.
[8] Abraham E, Grauby-Heywang C, Selector S, Jonusauskas G. Characterization of hemicyanine Langmuir–Blodgett films by picosecond time-resolved fluorescence. Journal of Photochemistry and Photobiology B Biology 2008;93:44–52.
[9] Naraoka R, Kaise G, Kajikawa K, Okawa H, Ikezawa H, Hashimoto K. Nonlinear optical property of hemicyanine self-assembled monolayers on gold and its adsorption kinetics probed by optical second-harmonic generation and surface plasmon resonance spectroscopy. Chemical Physics Letters 2002;362:26–30.
[10] Jedrzejewska B, Marciniak A, Paczkowski J. Studies on an argon laser-induced photopolymerization employing both mono- and bischromophoric hemicyanine dye–borate complex as a photoinitiator: Part II. Materials Chemistry and Physics 2008;111:400–8.
[11] Wang X-M, Zhou Y-F, Yu W-T, Wan C, Fang Q, Jiang M-H, et al. Two-photon pumped lasing stilbene-type chromophores containing various terminal donor groups: relationship between lasing efficiency and intramolecular charge transfer. Journal of Materials Chemistry 2000;10:2698–703.
[12] Wang XM, Wang D, Zhou GY, Yu WT, Zhou YF, Fang Q, et al. Symmetric and asymmetric charge transfer process of two-photon absorbing chromophores: bis-donor substituted stilbenes, and substituted styrylquinolinium and styrylpyridinium derivatives. Journal of Materials Chemistry 2001;11:1600–5.
[13] Qin CX, Zhou MY, Zhang WZ, Wang XM, Chen GQ. The synthesis and optical properties of three stilbene-type dyes. Dyes and Pigments 2008;77:678–85.
[14] Qin CX, Zhang WZ, Wang ZM, Zhou MY, Wang XM, Chen GQ. Optical properties of stilbene-type dyes containing various terminal donor and acceptor groups. Optical Materials 2008;30:1607–15.
[15] Ventelon L, Charier S, Moreaux L, Mertz J, Blanchard-Desce M. Nanoscale push–push dihydrophenanthrene derivatives as novel fluorophores for two-photon-excited fluorescence. Angewandte Chemie International Edition 2001;40:2098–101.
[16] Cao D-X, Liu Z-Q, Zhang G-H, Cao F-X, Chen H-Y, Li G-Z. Synthesis, structure and photophysical properties of three new hemicyanine dyes. Dyes and Pigments 2008;76:118–24.
[17] Wang XM, Yang P, Li B, Jiang WL, Huang W, Qian SX, et al. Two-photon absorption of new multibranched chromophore with dibenzothiophene core. Chemical Physics Letters 2006;424:333–9.
[18] Wang J, Cao W-F, Su J-H, Tian H, Huang Y-H, Sun Z-R. Syntheses and nonlinear absorption of novel unsymmetrical cyanines. Dyes and Pigments 2003;57:171–9.
[19] Narang U, Zhao CF, Bhawalkar JD, Bright FV, Prasad PN. Characterization of a new solvent-sensitive two-photon-induced fluorescent (aminostyryl) pyridinium salt dye. Journal of Physical Chemistry 1996;100:4521–5.
[20] Mansoor S-B, Said AA, Wei T-H, Hagan DJ, Van Stryland EW. Sensitive measurement of optical nonlinearities using a single beam. IEEE Journal of Quantum Electronics 1990;26:760–9.
[21] Karthikeyan B, Anija M, Suchand Sandeep CS, Muhammad Nadeer TM, Reji Philip. Optical and nonlinear optical properties of copper nanocomposite glasses annealed near the glass softening temperature. Optics Communications 2008;281:2933–7.
[22] Jedrzejewska B, Kabatc J, Paczkowski J. Dichromophoric hemicyanine dyes. Synthesis and spectroscopic investigation. Dyes and Pigments 2007;74:262–8.
[23] Choi DH, Wijekoon WMKP, Kim HM, Prasad PN. Second-order nonlinear optical effects in novel polymethacrylates containing a molecular-ionic chromophore in the side chain. Chemistry of Materials 1994;6:234–8.
[24] Cheng NL. Solvents Handbook (3rd version). Chemistry Industry Press; 2002. p. 198–981.
[25] Sarkar N, Das K, Nath DN, Bhattacharyya K. Twisted charge transfer process of Nile Red in homogeneous solution and in faujasite zeolite. Langmuir 1994;10:326–9.
[26] Krebs FC, Spanggaard H. An exceptional red shift of emission maxima upon fluorine substitution. Journal of Organic Chemistry 2002;67:7185–92.
[27] Ghazy R, Azim SA, Shaheen M, El-Mekawey F. Experimental studies on the determination of the dipole moments of some different laser dyes. Spectrochimica Acta Part A 2004;60:187–91.
[28] Mishra A, Behera RK, Behera PK, Mishra BK, Behera GB. Cyanines during the 1990s: a review. Chemical Reviews 2000;100:1973–2011.
[29] Sun J, Ren Q, Wang X-Q, Zhang G-H, Xu D. Study on nonlinear optical absorption properties of $[(CH_3)_4N]_2[Cu(dmit)_2]$ by *Z*-scan technique. Optics and Laser Technology 2009;41:209–12.
[30] Chen XB, Zhang JJ, Zhang HB, Jiang ZH, Shi G, Li YB, et al. Preparation and nonlinear optical studies of a novel thermal stable polymer containing azo chromophores in the side chain. Dyes and Pigments 2008;77:223–8.
[31] Zhang C, Song YL, Wang X, Kuhn FE, Wang YX, Xu Y, et al. Large third-order optical nonlinearity of two cubane-like clusters containing oxotrithiometalate anions and silver: synthesis, characterization, reactivity, and NLO properties–structure correlation. Journal of Materials Chemistry 2003;13:571–9.
[32] Li C, Shi G, Song YL, Zhang XL, Guang SY, Xu HY. Third-order nonlinear optical properties of Bi_2S_3 and Sb_2S_3 nanorods studied by the *Z*-scan technique. Journal of Physics and Chemistry of Solids 2008;69:1829–34.
[33] Qian SX, Zhu RY. Nonlinear Optics [M]. Fudan University Press; 2005. p. 111–5.